RSC Advances

ROYAL SOCIETY OF CHEMISTRY

www.rsc.org/advances

Table of Content

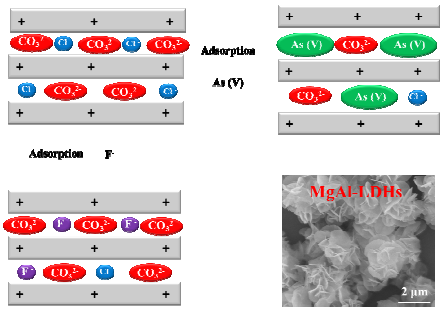

Three-dimensional hierarchical flower-like MgAl layered double hydroxides (MgAl-LDHs) with chloride and carbonate ions as interlayer anions showed excellent adsorption capacities for As (V) and F^- ions under neutral condition. Ion exchange mechanism between interlayer anions and As (V)/F^- ions was proposed.

Cite this: DOI: 10.1039/c0xx00000x

www.rsc.org/xxxxxx

ARTICLE TYPE

MgAl layered double hydroxides with chloride and carbonate ions as interlayer anions for removal of arsenic and fluoride ions in water

Pei-Pei Huang[a, b], Chang-Yan Cao*[a], Fang Wei[a], Yong-Bin Sun[a] and Wei-Guo Song*[a]

Received (in XXX, XXX) XthXXXXXXXXX 20XX, Accepted Xth XXXXXXXXX 20XX

DOI: 10.1039/b000000x

Layered double hydroxides (LDHs) are regarded as effective adsorbents to remove arsenic and fluoride ions in water. Compared to thorough researches of calcined LDHs, very few works were focused on the adsorption properties and mechanisms of LDHs themselves for these ions. In this manuscript, three-dimensional hierarchical flower-like MgAl layered double hydroxides (MgAl-LDHs) with chloride and carbonate ions as interlayer anions were synthesized via a solvothermal method without any surfactant. When tested as adsorbents for removal of As (V) and F^- ions, these hierarchical MgAl-LDHs showed maximum capacities of 125.8 and 28.6 $mg \cdot g^{-1}$, respectively, under neutral condition. The adsorption mechanisms for As (V) and F^- of hierarchical MgAl-LDHs were elucidated by X-ray diffractionpatterns, Fourier transformed infrared spectra, X-ray photoelectron spectroscopy and energy dispersive spectra. The results suggested that ion exchange between interlayer anions in hierarchical MgAl-LDHs and As (V) or F^- ions was the main adsorption mechanism. Chloride and carbonate ions intercalated in the MgAl-LDHs layers were exchanged with As (V), while only chloride ions were exchanged with F^- during adsorption.

Introduction

Arsenics and fluoride are serous health risk for many resodents in contaminated areas. Among various water treatment methods, adsorption may be one of the most adopt one.[1-14] Recently, layered double hydroxides (LDHs) and calcined LDHs (CLDHs) have been demonstrated as effective adsorbents to remove organic dyes and heavy metal anions due to advantages of low cost, thermal stabilities and excellent adsorption capacities.[15-21] The general formula of LDHs can be expressed as $[M^{II}_{1-x}M^{III}_{x}(OH)_2]^{x+}[A^{n-}_{x/n}]\bullet mH_2O$, where M^{II} and M^{III} are di- and trivalent metal cations in the octahedral positions of brucite-like layers, yielding excessive positive charge and A^{n-} represents an n-valent anion which balances the positive charges on the layers.[22] Among various morphologies, three-dimensional nanostructures that are composed of nanometer-sized building blocks show many advantages in adsorption.[23-28] Their nanometer-sized building blocks provide high surface area and active sites for adsorption and the overall micrometer-sized structure provides desirable mechanical strength and easy recovery. For example, Chen *et al.* reported a kind of SiO_2@LDH hierarchical spheres via ultrasound assisted direct growth of MgAl-LDH nanosheets on the surface of silica spheres for efficient removal of pharmaceutical waste from water.[29] Zhou prepared Li/Al-LDH with hierarchical porous structures by a hydrothermal method to remove fluoride ions.[19] However, only very few works reported about three-dimensional hierarchically LDHs and calcined LDHs.

Many previous works paid attention mainly on the removal of arsenate and fluoride ions over CLDHs, and the adsorption mechanism was mainly proposed to the structure reconstruction of CLDHs.[18,19,30-32] Yu *et al.* prepared 3D hierarchical flower-like MgAl-LDHs via a solvothermal method and they proposed that the main adsorption mechanism for As (V)/Cr (VI) removal was the structure reconstruction mechanism of MgAl-CLDHs.[31] Zhou reported that hierarchically porous Li/Al-CLDHs exhibited strong affinity towards fluoride via ion exchange, physical adsorption as well as insertion into the host layer lattice during the rehydration process.[19] However, very few works focused on the LDHs themselves, including adsorption properties and mechanisms.

Ion exchange (such as hydroxyl group, carbonate, and so on) is a dominant adsorption mechanism for removal of heavy metal ions from aqueous medium. Abundant interlayer anions within LDHs can also be exchanged and the adsorption properties are associated with the types of anions. For example, Wang *et al.* reported the interlayer nitrate ions in the Mg/Al-NO_3 LDHs could exchange with arsenate during adsorption process.[16] Kuroda *et al.* synthesized layered double hydroxide nanoparticles (LDHNPs) using a tripodal ligand of tris(hydroxymethyl)aminomethane, which displayed highly exchangeable capability of CO_3^{2-} that commonly regarded as impossible.[33]

In this study, we produced three-dimensional flower-like hierarchical MgAl layered double hydroxides (MgAl-LDHs) with chloride and carbonates ions as interlayer anions via a solvothermal method without any surfactant. These hierarchical MgAl-LDHs had a large surface area (95.7 $m^2 \cdot g^{-1}$) and showed excellent adsorption properties for As (V) and F^- with maximum capacities of 125.8 and 28.6 $mg \cdot g^{-1}$ under neutral condition, respectively. X-ray diffraction patterns, Fourier transformed infrared spectra, X-ray photoelectron spectroscopy and energy

dispersive spectra were used to investigate the adsorption mechanisms of hierarchical MgAl-LDHs for As (V) and F^-. The results showed that ion exchange between interlayer anions in hierarchical MgAl-LDHs and As (V) and F^- ions was the main adsorption mechanism. Chloride and carbonate ions intercalated in the MgAl-LDHs layers were exchanged with As (V), while only chloride ions were exchanged with F^- during adsorption.

Experimental Section

Materials

Analytical-grade magnesium chloride hexahydrate ($MgCl_2·6H_2O$), aluminum chloride hexahydrate ($AlCl_3·6H_2O$), urea, anhydrous methanol were purchased from Beijing Chemicals Co. (Beijing, China). Sodium hydrogen arsenate heptahydrate were purchased from Alfa Aesar. Sodium fluoride (ACS grade > 99 %) was purchased from Acros Organics. All chemicals were used without further purification. Deionized water used in all of the experiments was prepared using Milli-Qwater by Milli-Q system (Millipore, Bedford, MA).

Synthesis of MgAl-LDHs and MgAl-CLDHs

In a typical synthesis, $MgCl_2·6H_2O$, $AlCl_3·6H_2O$ and urea with a molar ratio of 2:1:7 were dissolved in 60 mL anhydrous methanol at room temperature. After stirred for 30 min, the clear solutions were transferred into a 100 mL autoclave, and then increased the temperature to 150 ℃ and kept for 6 h. The solid precipitate was collected by centrifugation and washed several times with water and ethanol, respectively. Finally, the product was dried at 80 ℃ for 12 h, denoted as MgAl-LDHs.

Characterizations

The microscopic features of the samples were characterized by scanning electron microscopy (SEM, JEOL-6701F), transmission electron microscopy (TEM, JEOL JEM-1011, 100 kV). X-Ray powder diffraction (XRD) patterns were collected on an X-ray diffractometer (Rigaku D/max-2500 diffractometer with Cu-Kα radiation, λ=0.154056 nm) at 40 kV and 200 mA. The surface area of the products was measured by the Brunauer–Emmett–Teller (BET) method using N_2 adsorption and desorption isotherms on an Autosorb-1 analyzer at 78.3 K. X-ray photoelectron spectroscopy (XPS) measurements were performed in a VG Scientific ESCALAB Mark II spectrometer equipped with two ultra-high vacuum (UHV) chambers. Fourier transformed infrared (FTIR) spectra were recorded on a Nicolet Magana-IR 750 spectrometer over a range from 400 to 4000 cm^{-1}. Metal elemental analysis was conducted using Inductively Coupled Plasma Atomic Emission Spectroscopy (ICP-AES, Shimadzu ICPE-9000). The concentration of fluoride was determined by ion chromatography (Dionex ICS-900) equipped with a AS-14A analytical column and a DS5 conductivity detector.

Adsorption experiments

Arsenate and fluoride solutions with different concentrations were prepared with $Na_2HAsO_4·7H_2O$ (98 %, Alfa) and NaF as the sources, respectively. All the initial solutions were adjusted to pH 7.0±0.1 using HCl (0.2 M). The batch adsorption experiments were carried out in 50 mL polyethylene tubes with 24 mg adsorbents and 30 mL arsenate or fluoride solutions of different concentrations at room temperature. After stirred for 24 h, the solutions were separated from suspensionsby centrifugation. Then the upper solutions filtered by 0.22 μm membrane were analyzed by ICP-AES or IC and the solids washed with deionized water twice and heated at 80 ℃ for 12 h for characterizations. The amount of special adsorbate ions adsorbed per unit weight of the adsorbent at equilibrium ($mg·g^{-1}$), q_e was calculated according to the following equation:

$$q_e=(C_0-C_e)V/m$$

where C_0 and C_e are the initial and equilibrium concentrations of adsorbate ions ($mg·L^{-1}$), respectively, V is the volume of the solution (L) and m is the mass of adsorbent (g).

Results and discussion

Characterizations of Flower-like MgAl-LDHs

Fig. 1a shows the typical SEM image of as-prepared MgAl-LDHs. They were composed of many uniform, three-dimensional hierarchical flower-like structures with a diameter of *ca.* 2-3 μm. The flower-like MgAl-LDHs were built of many nanosheets with the thicknesses of around 50-80 nm and connected to each other to form a highly open structure and no stand-alone plate-like LDHs could be seen. TEM images (Fig. 1b) further confirmed the hierarchical flower-like structures. Nanosheets were self-assembled to form flower-like nanostructures. EDS result (inset in Fig. S1) revealed the as-prepared MgAl-LDHs composed of Mg, Al, O, C and Cl. Particularly, Cl was detectable and the weight ratio was about 3.55 %. The typical X-ray diffraction (XRD) pattern of as-prepared MgAl-LDHs is shown in Fig. 1c. The diffraction peaks was in good agreement with characteristics of LDH-type materials reported in the literatures.[34-37] No other diffraction peaks can be found, indicating the purity of as-prepared MgAl-LDHs. The interlayer distance of MgAl-LDHs can be determined as 0.781 nm based on the (003) diffraction peak, which is larger than carbonate type LDHs.[17,30,31,38] This implied that there were also other anions co-existed in the interlayer. The FTIR spectrum of as-prepared MgAl-LDHs is shown in Fig. 1d. The strong peak at 3455 cm^{-1} was attributed to the vibration of hydroxyl groups associated with the interlayer water molecules and hydrogen bonding. The bands around 2956 cm^{-1} and 1066 cm^{-1} were assigned to the stretching vibrations of C–H and C–O from the solvent methanol, respectively.[39] The strong peak at 1385 cm^{-1} was attributed to the vibration mode of CO_3^{2-} in the interlayer of MgAl-LDHs. The bands in the range of 500−1000 cm^{-1} are attributed to M−O, O−M−O, and M−O−M lattice vibrations (M = Mg and Al). The surface area of flower-like MgAl-LDHs was tested by nitrogen adsorption-desorption (Fig. 2). The BET surface area was calculated to be 95.7 $m^2·g^{-1}$.

Based on the above results, we can conclude that chloride ions and carbonates ions were possibly co-exist as the interlayer anions. These anions in the interlayer were very important for the adsorption, which will be discussed in the following section.

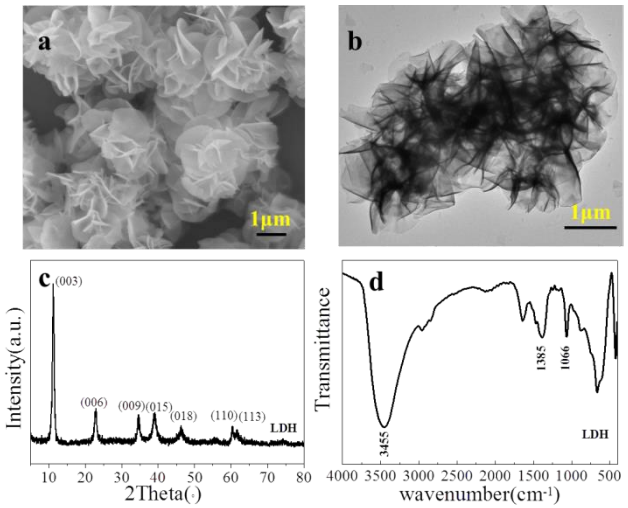

Fig. 1 (a) SEM image, (b) TEM image, (c) XRD pattern and (d) FTIR spectrum of as-prepared MgAl-LDHs.

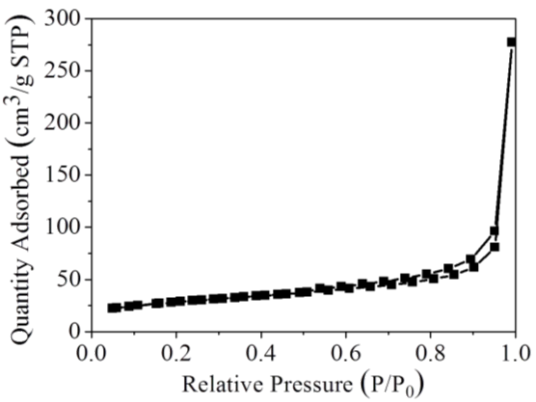

Fig. 2 Nitrogen adsorption and desorption isotherms of MgAl-LDHs

Adsorption Properties of Flower-like MgAl-LDHs

In order to investigate the adsorption process over hierarchical MgAl-LDHs, adsorption isotherms are obtained with initial concentrations of As (V) and F^- ranging from 10 to 200 mg/L. Fig. 3 shows the adsorption isotherms of As (V) and F^- ions over MgAl-LDHs. The adsorption data were fitted with both Langmuir and Freundlich models.

The Langmuir model is applicable for uniform adsorption processes, where each adsorption site on the surface has identical binding sites and is described as monolayer adsorption.[40] Langmuir model can bedescribed as follows:

$$q_e = q_m b C_e/(1+bC_e)$$

where C_e (mg·g^{-1}) and q_e (mg·g^{-1}) are the equilibrium concentration of adsorbate ions in the supernatant and the amount of adsorbate ions adsorbed on per weight of LDHs at equilibrium, respectively. q_m (mg·g^{-1}) is the maximum adsorption capacity associated with complete monolayer coverage, and b (L·mg^{-1}) is a Langmuir constant related to the energy and affinity of the sorbent.

The Freundlich model is an empirical description of adsorption on heterogeneous surface and expressed as: [41]

$$q_e = K_F C_e^{1/n}$$

where C_e is the equilibrium concentration of adsorbate ions (mg·L^{-1}), q_e is the amount of adsorbate ions adsorbed per unit weight of the adsorbent at equilibrium (mg·g^{-1}), K_F is the empirical constant (L·mg^{-1}) and n is the empirical parameter related to the adsorption intensity.

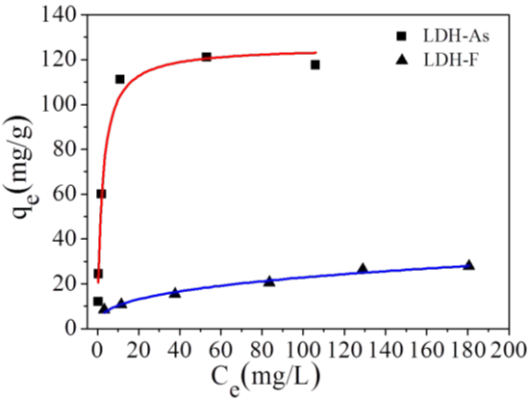

Fig. 3 Adsorption isotherms of arsenate/fluoride on the MgAl-LDHs.

The detailed fitting parameters of the Langmuir and Freundlich models are listed in the Table S1. It can be seen that the adsorption data of MgAl-LDHs for As (V) was fitted better with Langmuir model than Freundlich model, while opposite for adsorption of F^- ions. The maximum adsorption capacities of as-prepared MgAl-LDHs for As (V) and F^- were 125.8 and 28.6 mg g^{-1}, respectively. These adsorption capacities were obtained at pH ≈ 7.0, which is similar to the real underground water condition.

Adsorption Mechanisms of Flower-like MgAl-LDHs for As (V) and F^-

To investigate the detailed adsorption mechanisms for arsenic and fluoride, As (V) and F^- saturated flower-like MgAl-LDHs nanostructures were prepared. After adsorption, the solid samples were centrifugated and washed with water for several times, and then dried for characterizations. The adsorption mainly occurred on the surface. Therefore, XPS was used to characterize the surface states of flower-like MgAl-LDHs before and after adsorption of arsenic and fluoride. As shown in Fig. 4a, arsenic signal appeared after adsorption, suggesting As (V) ions were successfully adsorbed on flower-like MgAl-LDHs. However, the peak of Cl 2p at 198 eV disappeared after As(V) adsorption. This suggested that chloride may exchange with As(V). EDS result after As (V) adsorption also showed that As (V) ions were adsorbed and chloride ions were almost not detected (Fig. S2).

Besides, the high resolution C1s spectra of LDHs before and after As(V) adsorption (inset in the Fig. 4a) shows that the intensity of carbonate located at 288.4 eV, which could be assigned to the intercalated CO_3^{2-} of MgAl-LDHs, decreases significantly after As(V) adsorption, indicating that the partial replacement of interlayer CO_3^{2-} was also exchanged with As(V). FTIR spectrum of MgAl-LDHs after As (V) adsorption is shown in Fig. S3. As we can see, the intensity of the band located at 1385 cm^{-1} of interlayer carbonate was considerably decreased after adsorption of As (V) for MgAl-LDHs. At the same time, a new band of As-O stretching vibration located at 852 cm^{-1} was detected, further confirming the ionexchange of carbonate with

As(V) occurred. [42,43]

Fig. 4b shows the XPS spectra of MgAl-LDHs before and after fluoride adsorption. Fluoride peak appeared and the peaks at 198 eV (Cl 2p) and 267 eV (Cl 2s) disappeared after fluoride adsorption, indicating ion exchange between chloride and fluoride occurred. EDS result confirmed no detectable chloride was observed in MgAl-LDHs after fluoride adsorption (Fig. S4). The high resolution of F 1s spectrum is shown in the inset of Fig. 4b. The small peak at 685 eV and the main peak at 689.3 eV can be assigned to physically adsorbed F^- on the surface and F^- in the lattice of MgAl-LDHs, respectively.[19,44,45] This results suggested that fluoride ions mainly intercalated into the layers other than adsorbed on the surface. In addition, no obvious change of C1s spectra was observed of MgAl-LDHs before and after fluoride adsorption, indicating carbonate ions may not participated in the ion exchange during fluoride adsorption.

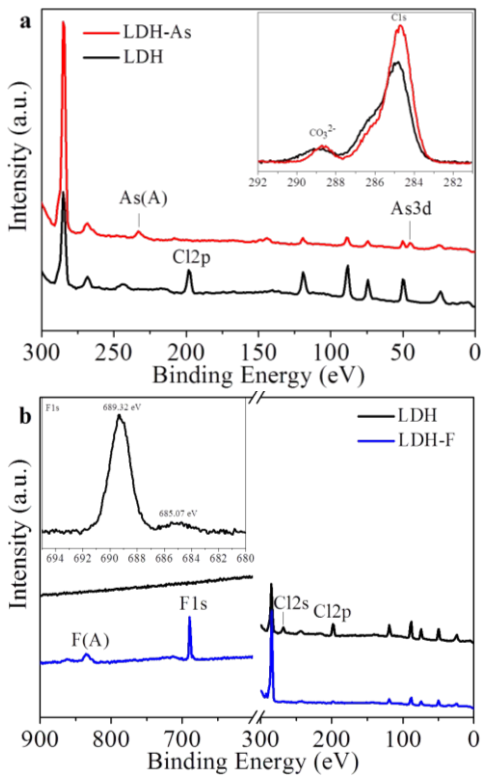

Fig. 4 XPS spectra of MgAl-LDHs before and after adsorption of (a) As (V) and (b) F^-.

SEM images of MgAl-LDHs after adsorption of As (V) and F^- ions showed that the structures could be maintained (Fig. S5). XRD patterns of as-prepared MgAl-LDHs after adsorption of As (V) were shown in Fig. 5a. No obvious change of the interlayer spacing of as-prepared flower-like MgAl-LDHs was detected at low concentrations. However, obvious shift of the interlayer spacing to a higher diffraction angle was observed at high concentrations, indicating that As (V) intercalated into the interlayer and expanded the interlayer. While for fluoride adsorption (Fig. 5b), nearly no change can be seen with full range of concentrations. This was because only chloride ions were exchanged with fluoride ions and nearly the same size of them.

Based on the above results, ion exchange between interlayer anions in hierarchical MgAl-LDHs and As (V) and F^- ions in solution was the main adsorption mechanism. Chloride and carbonate ions intercalated in the MgAl-LDHs layers were exchanged with As (V), while only chloride ions were exchanged with F^- during adsorption.

In general, MgAl-LDHs have greater affinity for multivalent inorganic anions compared with monovalent inorganic anions. The affinity has been reported to decrease in the order CO_3^{2-} > SO_4^{2-} > F^- > Cl^- > NO_3^-,[46] which is consistent with our experimental results. Based on this order, the fact in this work that chlorides, carbonates intercalated in the LDHs layers were exchanged with As (V) while only chlorides were exchanged with fluorides during adsorption could be explained. The fact that only Cl^- was involved in F^- adsorption, while both Cl^- and CO_3^{2-} were involved in As (V) adsoprtion is worth investigation, as it was related to the distribution of anions in the clay layer, and how guest anions can enter the inter layer space.

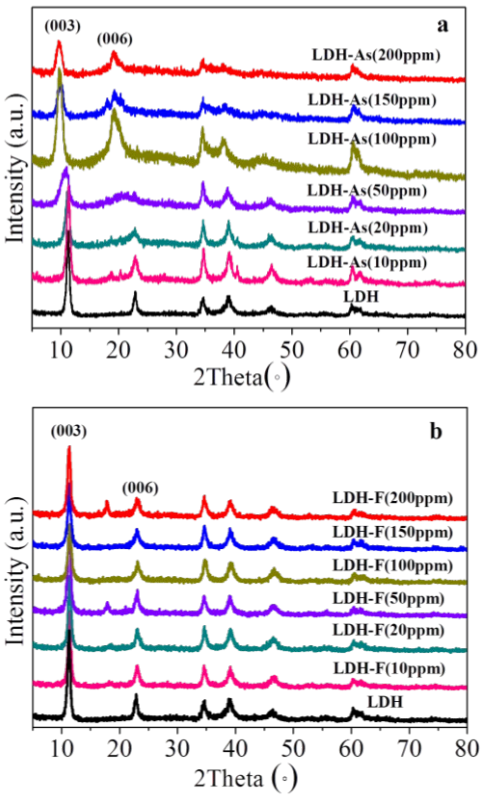

Fig. 5 XRD patterns of MgAl-LDHs after adsorption of (a) As (V) and (b) F^- with different initial concentrations.

Conclusions

Three-dimensional hierarchical MgAlLayered double hydroxides (MgAl-LDHs) with carbonate and chloride ions as the interlayer anions were produced by a solvothermal method without adding surfactant. These hierarchical MgAl-LDHs showed excellent adsorption properties for As (V) and F^- with maximum capacities of 125.8 and 28.6 mg g^{-1} under neutral condition, respectively. Ion exchange between interlayer anions in hierarchical MgAl-LDHs and As (V) and F^- ions was the main adsorption mechanism, which was very different from the structure reconstruction mechanism of calcined MgAl-LDHs. Chloride and carbonate ions intercalated in the as-prepared

MgAl-LDHs layers were exchanged with As (V), while only chloride ions were exchanged with F^- during adsorption.

Acknowledgements

We thank the financial support from the National Basic Research Program of China (2011CB933700, 2012BAJ25B08), the National Natural Science Youth Foundation of China (NSFC 51402305) and the Chinese Academy of Sciences (XDA09030200, GJHZ1224, KJCX2-YW-N41).

Notes and references

[a]*Beijing National Laboratory for Molecular Sciences (BNLMS)& Key Laboratory of Molecular Nanostructure and Nanotechnology, Institute of Chemistry, Chinese Academy of Sciences, Beijing, 100190, People's Republic of China*
E-mail: cycao@iccas.ac.cn, wsong@iccas.ac.cn.
[b]*University of Chinese Academy of Sciences, Beijing 100049, People's Republic of China*

† Electronic Supplementary Information (ESI) available: [EDS and FTIR spectra of MgAl-LDHs before and after adsorption of As (V) and F^-, and table of summary of the Langmuir and Freundlich isotherm model parameters for the As(V)/F- uptake capacity on LDHs]. See DOI: 10.1039/b000000x/

References

1 D. Mohan, C. U. Pittman, Jr., *J.Hazard.Mater.*, 2007, **142**, 1.
2 X. Zhuang, Y. Wan, C. M. Feng, et al., *Chem. Mater.*, 2009, **21**, 706.
3 A. Bhatnagar, E. Kumar, M. Sillanp ää, *Chem. Eng. J.*, 2011, **171**, 811.
4 G. X. Zhao, J. X. Li, X. M. Ren, et al., *Environ. Sci. Technol.*, 2011, **45**, 10454.
5 H. W. Liang , X. Cao , W. J. Zhang, et al., *Adv. Funct. Mater.*, 2011, **21**, 3851.
6 W. Li, C. Y. Cao, L. Y. Wu, et al., *J. Hazard. Mater.*, 2011, **198**, 143.
7 H. W. Liang, Q. F. Guan, L. F. Chen, et al., *Angew. Chem. Int. Ed.*, 2012, **51**, 5101.
8 B. Wang, H. B. Wu, L. Yu, et al., *Adv. Mater.*, 2012, **24**, 1111.
9 C. Y. Cao, J. Qu, W. S. Yan, et al.. *Langmuir*, 2012, **28**, 4573.
10 Z. X. Wu, W. Li, P. A. Webley, et al., *Adv. Mater.*, 2012, **24**, 485.
11 J. Qu, C. Y. Cao, W. Li, et al., *J. Mater. Chem.*, 2012, **22(33)**, 17222.
12 H. Chen, J. X. Li, X. L. Wu, et al., *Ind. Eng. Chem. Res.* 2014, **53,** 16051.
13 H. J. Yu, Y. Y. Lv, K. Y. Ma,et al., *J. Colloid Interface Sci.*, 2014, **428**, 251.
14 X. M. Zhang, J. Y. Liu, Sean Joseph Kelly, et al., *J. Mater. Chem. A*, 2014, **2**, 11759.
15 K. Mandel, A. Drenkova-Tuhtan, F. Hutter, et al., *J. Mater. Chem. A*, 2013, **1**, 1840.
16 S. L. Wang, C. H. Liu, M. K. Wang, et al., *Appl. Clay Sci.*, 2009, **43**, 79.
17 T. Wen, X. L. Wu, X. L. Tan, et al., *ACS Appl.Mater.Interfaces*, 2013, **5**, 3304.
18 Y. F. Xu, Y. C. Dai, J. Z. Zhou, et al., *J. Mater. Chem.*, 2010, **20**, 4684.
19 J. B. Zhou, Y. Cheng, J. G. Yu, et al., *J. Mater. Chem.*, 2011, **21**, 19353.
20 X. L. Wu, X. L. Tan, S. T. Yang, et al., *Water Res.*, 2013, **47**, 4159.
21 L. C. Tan, Y. L. Wang, Q. Liu, et al., *Chem. Eng. J.*, 2015, **259**, 752.
22 P. Gunawan, R. Xu, *Chem. Mater.*, 2009, **21**,781.
23 L. S. Zhong, J. S. Hu, A.M. Cao, et al., *Chem. Mater.*, 2007, **19**, 1648.
24 J. S. Hu, L.S. Zhong, W.G. Song, et al., *Adv. Mater.*, 2008, **20**, 2977.
25 H. Li, W. Li, Y. J. Zhang, et al., *J. Mater. Chem.*, 2011, **21**, 7878.
26 J. Qu, C. Y. Cao, Y. L. Hong, etal., *J. Mater. Chem.*, 2012, **22**, 3562.
27 C. Y. Cao, J. Qu, F. Wei, et al., *ACS Appl. Mater. Interfaces*, 2012, **4**, 4283.
28 S. W. Zhang, J. X. Li, T. Wen, et al., *RSC Advances*, 2013, **3**, 2754.
29 C. P. Chen, P. H. Wang, T.T. Lim, et al., *J. Mater. Chem. A*, 2013, **1**, 3877.
30 L. Lv, J. He, M. Wei, et al., *J. Hazard.Mater.*, 2006, **133**, 119.
31 X. Y. Yu, T. Luo, Y. Jia, et al., *Nanoscale*, 2012, **4**, 3466.
32 K. H. Goh, T. T. Lim, Z. L. Dong, *Water Res.*, 2008, **42**, 1343.
33 Y. Kuroda, Y. Miyamoto, M. Hibino, et al., *Chem. Mater.*, 2013, **25**, 2291.
34 E. Gardner, K. M. Huntoon, T. J. Pinnavaia, *Adv. Mater.*, 2001, **13**, 1263.
35 B. Li, J. He, *J. Phys. Chem. C*, 2008, **112**, 10909.
36 J. G. Wang, Y. Wei, J. Yu, *Appl. Clay Sci.*, 2013, **72**, 37.
37 Z. P. Xu, G. Q. Lu, *Chem. Mater.*, 2005, **17**, 1055.
38 A. G. Caporale, M. Pigna, J. J. Dynes, et al., *J. Hazard. Mater.*, 2011, **198**, 291.
39 J. A. Gursky, S. D. Blough, C. Luna, et al., *J. Am. Chem. Soc.*, 2006, **128**, 8376.
40 I. Langmuir, *J. Am. Chem. Soc.*, 1916, **38**, 2221.
41 H. Freundlich, *Z. Phys. Chem.*, 1906, **57**, 385.
42 N. Mahanta, J. P. Chen, *J. Mater. Chem. A*, 2013, **1**, 8636.
43 S. V. Prasanna, P. V. Kamath, *J. Colloid Interface Sci.*, 2009, **331**, 439.
44 J. G. Yu, W. G. Wang, B. Cheng, et al., *J.Phys.Chem. C*, 2009, **113**, 6743.
45 Y. L. Tang, X. H. Guan, J. M. Wang, et al., *J. Hazard. Mater.*, 2009, **171**, 774.
46 S. Miyata, *Clay Clay Miner.*, 1983, **31**, 305.